Tectonics

RESEARCH ARTICLE
10.1029/2020TC006493

Key Points:

- New insights into the lateral-strength variations and depth to the brittle-ductile transition zone
- Tectonic implications of the seismic activity in NW Iberia
- Mechanisms of brittle failure and depth variations to the brittle-ductile transition zone in NW Iberia

Correspondence to:
J. Fernández-Lozano,
jferl@unileon.es

Citation:
Fernández-Lozano, J., Martín-González, F., & De Vicente, G. (2021). New insights into the lateral-strength variations and depth to the brittle-ductile transition zone in NW Iberia. *Tectonics*, *40*, e2020TC006493. https://doi.org/10.1029/2020TC006493

Received 22 AUG 2020
Accepted 14 JAN 2021

New Insights into the Lateral-Strength Variations and Depth to the Brittle-Ductile Transition Zone in NW Iberia

J. Fernández-Lozano[1], F. Martín-González[2], and G. De Vicente[3,4]

[1]Prospecting and Mining Research Area, Department of Mining, Topography and Structure Technology, Higher Technical School of Mining Engineering, León, Spain, [2]Área de Geología-ESCET, Universidad Rey Juan Carlos, Móstoles, Madrid, Spain, [3]GEODESPAL Faculty of Geology, Complutense University of Madrid, Spain, [4]Institute of Geosciences IGEO, UCM-CSIC, Madrid, Spain

Abstract The northwest of Iberia experiences important tectonic activity that has led to several episodes of seismic swarms. Despite substantial knowledge of the surface structures that could be responsible for this activity, their distribution at depth remains unclear. Geophysical research and rheological data display important discrepancies concerning the deep structure of the area. In order to shed light on the processes that control deep seismicity and their relationship with surface structures, we combine the analysis of seismic activity in northwest Iberia with the interpretation of sandbox experiments simulating tectonic structures similar to those observed. The structural interpretation of the modeling results was conducted by analyzing the surface particle image velocimetry field. Additionally, yield strength and brittle-ductile transition zone (BDTZ) maps were constructed from model sections. The modeling results show a direct relationship between the main active structures developed along pre-existing weak zones and the observed variations in crustal thickness. Moreover, these thickened zones correspond to the sectors where the BDTZ in the crust deepens. Therefore, the anomalous thickness and lateral variations of the seismogenic zone cannot be solely explained by rheological or structural changes but result from a combination of factors such as fluid pressure and the location of fractures at depth, which controls the fluid migration responsible for the failure of crustal faults. These factors can trigger seismic activity at depth and may control the observed thickness variations in the BDTZ.

1. Introduction

The mechanism of faulting is controlled by pressure, temperature, fluid pressure, and strain-rate leading to brittle fracture and frictional slip in the upper levels of the continental crust, and ductile flow at greater depths (Pollard & Fletcher, 2005; Tullis & Yund, 1977). The transition from one domain to the other is defined by the brittle-ductile transition zone (BDTZ), which also represents the transition between the rheological changes from cataclasis to crystal plasticity (e.g., Stewart et al., 2000). This boundary demarcates the limit of the seismogenic zone (with 95% of all seismicity, Magistrale, 2002). This sharp level correlates to the depth to which earthquakes occur in the continental interiors due to the rapid reduction of resistance to shearing (e.g., Long & Zelt, 1991; Sibson, 2007). This boundary is controlled by factors affecting the deformation mechanisms, such as temperature, pressure, strain rate, composition, pore fluid pressure, and tectonic stress (Stewart et al., 2000; Tullis & Yund, 1977). Variations in these factors are responsible for changes of the BDTZ depth and therefore the thickness of the seismogenic crust (Figure 1a).

In most tectonic regions, earthquakes are occurring in the shallow part of the lithosphere (C. Scholz, 1988), where rock strength is mostly controlled by thermo-mechanical properties (i.e., rheology and thermal gradient), crustal thickness and rock composition (Maggi et al., 2000; Watts & Burov, 2003). Early observations of brittle-plastic transition provide evidence of increasing plastic flow with depth and the progressive change in the physical factors that control rock deformation (Sibson, 1977). The BDTZ represents a transition in which semi-brittle deformation dominates (C. H. Scholz, 2002). This shift constrains the maximum depth at which earthquakes can occur and represents a mixture of brittle and plastic processes at the microscale, while the rheology is macroscopically ductile (Karato, 2012; C. Scholz, 1988).

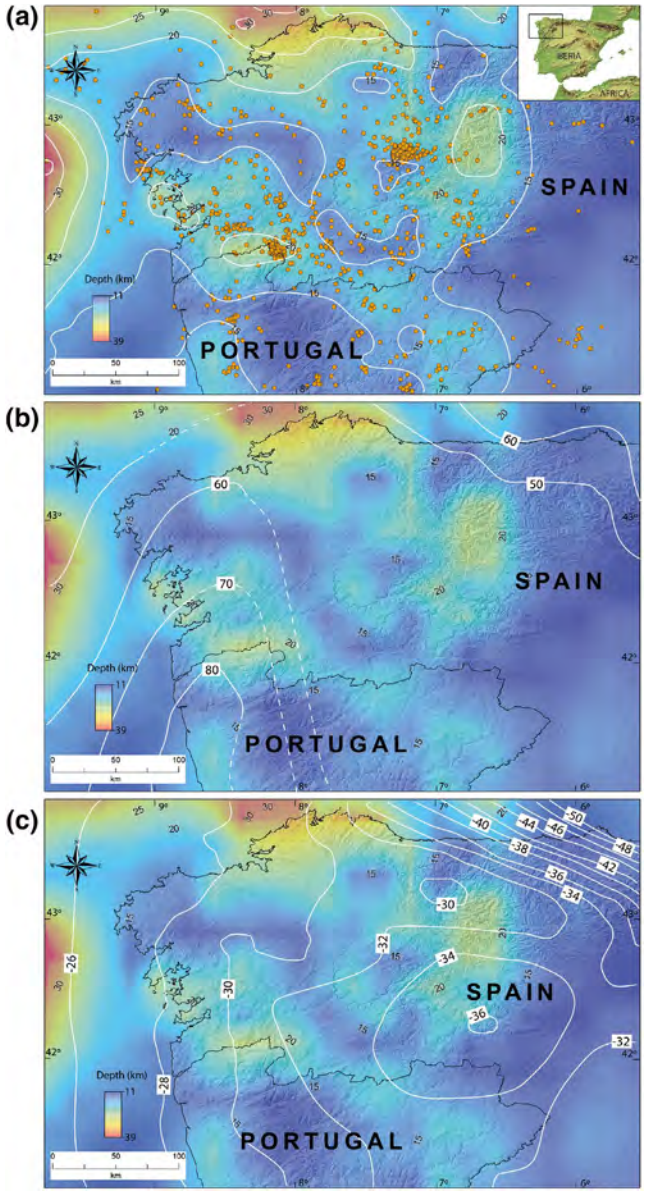

Figure 1. Brittle-ductile transition zone maps obtained from interpolation of earthquakes data (notice that the eastern sector comprises a wide area across the Cantabrian Mountains with little or no seismicity) including the following: (a) seismic epicenters; (b) heat flow data in mW/m^2 (Fernández et al., 1998), and (c) crustal thickness in km (Gallastegui, 2000) .

In northwest (NW) Iberia, Llana-Fúnez and López-Fernández (2015) deduced the thickness of the seismogenic zone through the analysis of crustal-scale rheological profiles based on geological parameters (e.g., temperature, pressure, strain rate, composition, and tectonic regime). For instance, heat flow can control the depth of the BDTZ. Thus, a higher geothermal gradient would reduce its thickness. Heat flow data in the specific area are heterogeneously distributed, showing important variations across strike (Duque, 2020; Fernández et al., 1998; Marzán, 2000) (Figure 1b). In general terms, NW Iberia reaches 60–80 mW/m^2 in the southwest of the region decreasing toward the east to 50 mW/m^2 in the Cantabrian Mountains. This would mean a reduction in brittle crustal thickness to the southwest when compared with the Cantabrian Mountains area, which is in contradiction with what is observed in the BDTZ, where the thicker seismogenic crust is located in the southwest. This could suggest that hot fluids can be channeled by the numerous faults in the area reducing the rock strength and producing subsequent seismicity.

According to Llana-Fúnez and López-Fernández (2015), the brittle-ductile transition is expected to be between 10 and 16 km depth (Figure 1a). However, this model does not fit with previous studies that suggest the brittle-ductile transition zone shows this boundary to be at 20 km depth, with a Moho depth between 28 and 35 km (Díaz et al., 2009; Fernandez-Viejo et al., 2000; Gallastegui, 2000). The general trend for the crustal thickness shows a westward decrease, reaching offshore around 26 km, being the thickest under the main relief of the Cantabrian Mountains (>40 km) and the Galician-Leonese Mountains (36 km) (Gallastegui, 2000). This distribution does not correlate with the seismogenic thickness, given its important thickening in the west (Figure 1c). These authors ascribed the excessive thickness of the seismogenic zone to a wide number of reasons, considering: (i) the BDTZ as the boundary between the upper and lower crust based on a significant change in rock mechanics; (ii) the lithological and tectonic variations at upper mid-crustal levels, and (iii) the deep Alpine structure of the Cantabrian orogen changing from east to west (i.e., the effect of lower crust indentation). For instance, they invoked variations in fluid pressure, and locally; in the seismic clusters of Sarria-Triacastela-Becerreá, a certain degree of heating of host rocks. The influence of these rheological factors was reported to affect the seismic behavior of the crust (Karato, 2012; C. H. Scholz, 2002). Alternatively, deep seismic reflection and refraction data suggest that this transition in the upper and lower crust occurs in Iberia at depths of 12–20 km (Fernández-Viejo et al., 2000; Pérez-Estaún et al., 1994; Simancas et al., 2003), based on the interpretation of a series of reflectors that have interpreted in different ways: the presence of a middle crust, subhorizontal fault planes, layered intrusions, the presence of fluids, and mineral phase changes within different intraplate scenarios, etc. (Gans et al., 1985; Gougb, 1986; Simancas et al., 2003). Although significant progress has been made to relate surface observations to the crustal structure of the Iberian lithosphere, the transition between seismic and aseismic behavior in the crust, the fault kinematics, and the presence of dispersed seismicity over a relatively stable plate interior in NW Iberia remains unclear, attracting the interest of the scientific community (e.g. Llana-Fúnez & López-Fernández, 2015; López-Fernández et al., 2012; Martín-González et al., 2012; Martínez-Díaz et al., 2006).

Here, we provide new insights into the thickness and the lateral-strength variation of the BDTZ in NW Iberia (Figure 1). To do so, a comparison of surface topography, heat flow and crustal thickness, seismic-

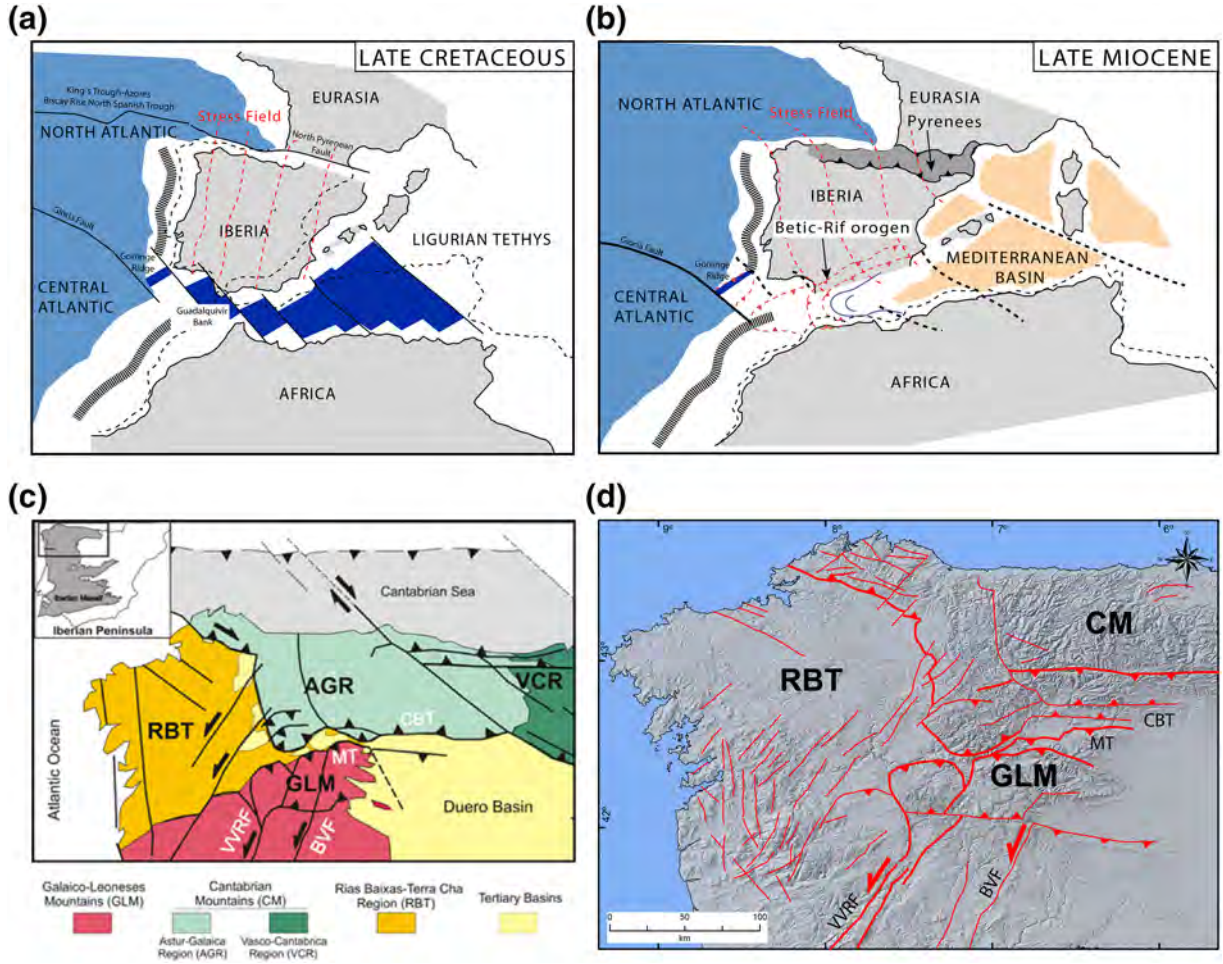

Figure 2. a) Paleogeographic reconstruction showing the Late Cretaceous early convergence position of Iberia; (b) its Late Miocene configuration sandwiched between Africa and Europe (Redrafted from Vergés et al. (2019); (c) Structural sketch showing the different tectono-stratigraphic regions of the Western part of the Alpine Pyrenean-Cantabrian Orogen in the northern Iberian Peninsula (modified from Martín-González & Heredia, 2011a), and (d) Structural map que the main Alpine structures in the NW Iberia, compilated from the Spanish Geological Survey maps (GEODE) and Martín-González and Heredia (2011a).

ity, and tectonic style from the study area with crustal cross-sections obtained from analog experiments was carried out. Our analysis of fault kinematics reconciles intraplate mountain building and strain localization with the observed structure of the deep interior of the Earth. Modeling results suggest that the BDTZ is characterized by the presence of Alpine tectonic structures that led to the anomalous thickness of the seismogenic crust. We believe that it is due to the presence of build-in fluid pressure related to the location of fault planes at depth. High pore fluid pressures are likely responsible for shear stresses exceeding the yield strength of the crust, giving rise to significant seismic activity in the area. Analog experiments also provide an excellent template to understand the depth variations observed along the BDTZ within intraplate areas otherwise inaccessible to direct observation.

2. Geological Setting

The NW Iberian Peninsula is part of a Variscan basement (Iberian Massif) mainly made of Paleozoic igneous and metamorphic rocks deformed during the Variscan Orogeny (e.g., Martínez-Catalán et al., 1997; Perez-Estaún et al., 1994). The Alpine deformation that gave rise to the Alpine Pyrenean-Cantabrian Orogen resulted from the oblique convergence and collision of the Iberian and the Eurasian Plates from Late Cretaceous to Early Miocene during the compressional stage of the Alpine cycle (Figures 2a and 2b) (Dewey et al., 1989; Rosenbaum et al., 2002; Vergés et al., 2002). The Alpine Pyrenean-Cantabrian

Orogen trends east-west and comprises the Pyrenees in the east and the Cantabrian Mountains to the west (Gallastegui et al., 2000; Muñoz, 2002; Martín-González & Heredia, 2011a).

The Cantabrian Mountains, in turn, can be divided into two tectonic regions (Figure 2c): the Vasco-Cantabrian Region in the east and the Astur-Galaica Region in the west (Martín-González & Heredia, 2011a and references therein). In the latter, the Alpine deformation reactivated Variscan structures (de Vicente et al., 2008; Fernández-Lozano et al., 2019; Vegas et al., 2004), and the Cenozoic synorogenic sediments (Oligocene-Lower Miocene) resulted from an eroded broken foreland basin (Martín-González & Heredia, 2011b). Therefore, the NW Iberian Peninsula can be subdivided into the Cantabrian Mountains, the Galaico-Leonese Mountains, and the Rias Baixas-Terra Cha Region (Figure 2c).

The Alpine collision of the Iberian and the European plates (e.g., Muñoz, 2002; Roca et al., 2011; Vergés et al., 2002) controlled the reactivation styles from east to west (e.g., Fernández-Lozano et al., 2019; Gallastegui et al., 2000; Martín-González & Heredia, 2011a; Pulgar et al., 1996; Roca et al., 2011). The Maximum Horizontal Shortening (Shmax) during the Eocene to early Miocene was N-S (Andeweg, 2002; de Vicente et al., 2008) and the amount of shortening accommodated during the Alpine collision is higher in the Pyrenees (Figure 2a) (between 150 and 90 km, decreasing to the west) (Alonso et al., 1996; Muñoz, 2002). After late Miocene (Figure 2b), the Iberian plate detaches from Africa to form part of the Eurasian plate, leading to the present-day mountain configuration (De Vicente & Vegas, 2009), by a shift in the orientation of the maximum stress orientations to SE-NW (Figure 2d).

One of the main characteristics of NW Iberia is that it constitutes the Western termination of the Alpine Pyrenean-Cantabrian Orogen reliefs (Martín-González & Heredia, 2011a; Santanach, 1994). The main Alpine structure of the Cantabrian Mountains is a regional monocline related to a major fault-bend fold, related to the so-called Cantabrian Basal Thrust (CBT) (Alonso et al., 1996) (Figure 2). The CBT is an E-W striking, north-dipping thrust responsible for the uplift of the Cantabrian Mountains, crustal thickening and the modification of the BDTZ. However, in the westernmost termination, the relief splits in two: the Galaico-Leonese Mountains and the Cantabrian Mountains (Ancares) (Figures 2c and 2d). The relief of the later is uplifted mainly by north dipping thrust faults and faulting propagates westward from Eocene to late Oligocene (Martin-González et al., 2014). Meanwhile, in the south, the Galaico-Leonese Mountains relief is subsequently uplifted by south-dipping thrusts, active mainly during the Miocene and Late Miocene, when the plate boundary changed toward southern Iberia (Martin-Gonzalez et al., 2012b). There, especially in the south and southwest, a set of NNE-SSW strike-slip faults connect with the main compressional structures (Martin González et al., 2012a) (Figure 2). These strike-slip faults are Late-Variscan in age and accommodated part of the Alpine shortening. They registered their main activity after the middle Miocene, when the orientation of the maximum stress orientation shifted from NS to NW (Betic stage), leading to present-day seismicity along the Bragança-Vilariça (also called Manteigas-Vilariça-Bragança), Verín-Vila Real (also called Penacova-Regua-Verín) and Monforte-Orense fault corridors, (Cabral, 1989; De Vicente & Vegas, 2009; Martín-González et al., 2012a; Ribeiro et al., 1990; Rockwell et al., 2009).

In the last few years, geological, geophysical, and petrological information has provided useful information on the deep structure of the Iberian plate interior (Figure 1) (De Lis Mancilla & Diaz, 2015; De Vicente et al., 2007; Díaz & Gallart, 2009; Díaz et al., 2009, 2016; Fernández-Viejo et al., 2000; Jiménez-Díaz et al., 2012; Pérez-Estaún et al., 1994; Suriñach & Vegas, 1988; Simancas et al., 2003). The seismic structure of the crust in NW Iberia is represented by a three-layered system comprising: (i) an upper-crust level reaching 12 km with seismic velocities between 5.6 and 6 km/s; (ii) a middle crust layer with velocities varying between 6.2 and 6.3 km/s extending to 22 km; and (iii) a lower crust with velocities ranging from 6.6 to 6.9 km/s and reaching the Moho discontinuity at 30–32 km (Córdoba et al., 1988; Díaz et al., 2009; Fernández-Viejo et al., 2000; Rodríguez-Fernández et al., 2015).

Table 1
Sandbox Experiment Parameters

Brittle crust	Nature	Model
Density	2750	1300
Gravity	9.81	9.8
Thickness	15000	0.015
Cohesion	0	35
internal friction	0.7	0.7
Deviatoric stress (shortening)	7.60 E+08	429.114093959732
Ductile crust	Nature	Model
Gravity	9.81	9.81
Length (thickness) (m)	20000	0.0200
Density (kg/m3)	2900	1356
Viscosity Pa/sec	4.50 E+21	3.53 E+04
Velocity m/s	4.75646879756469E-11	2.78E-06
Ramberg Number		Smoluchowski Number
Nature	Model	Nature	Model
53.1654912	54.2446079347549	0.028571428571429	0.003849444

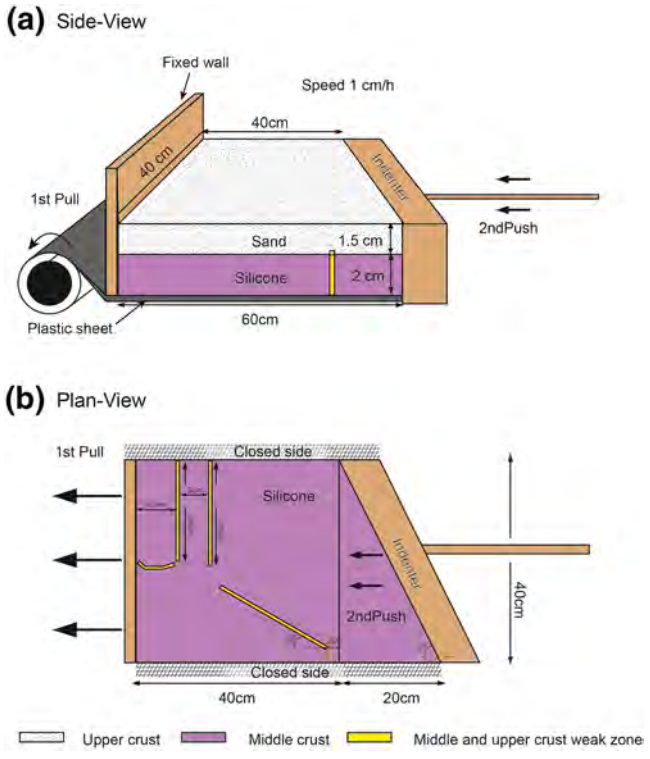

Figure 3. Experimental set-up of the sandbox experiment shown in this work. (a) Model side-view and (b) Model plan-view.

3. Material and Methods

A two-layer sandbox experiment was performed to test the mechanical behavior of the crust during deformation. The analog modeling results were analyzed with the velocity field analysis (particle image velocimetry [PIV]) carried out over the surface of the models and the BDTZ analysis maps.

3.1. Analog Modeling

The experimental set-up was constrained by a broad range of geological and geophysical data that allowed us to constrain material properties, layer thickness, velocity of deformation, and total bulk shortening (Díaz et al., 2009; Fernández-Viejo et al., 2000; Martín-González, 2009; Martín-González & Heredia, 2011a; Rodríguez-Fernández et al., 2015). The experiments were performed in a sandbox with a two-layer crust (upper and middle-lower crust, 1.5 and 2.0 cm, respectively), 16% shortening and velocity rate of 10 mm/h (see Table 1).

The model crust was characterized by brittle/viscous rheological stratification. A brittle upper crust composed of a mixture of Quartz and Feldspar sands, and a ductile middle-lower crust represented by a silicone putty layer (models set-up and material properties are shown in Figure 3 and Table 1). Four weak zones representing pre-existing Late-Variscan fault systems in NW Iberia were incorporated. They comprised a low-viscosity Newtonian silicone band representing: (i) the E-W Cantabrian Mountains and the Galaico-Leonese Mountains; (ii) the NNE-SSW Verín-Vila Real Fault and the Bragança-Vilariça Fault, and (iii) a curved weak zone that represented the Cantabrian Arc. These silicone strips were included in the lower crust silicone and the bottom of the sand layer (see the model set-up in Figure 3 and Ta-

10.1029/2020TC006493

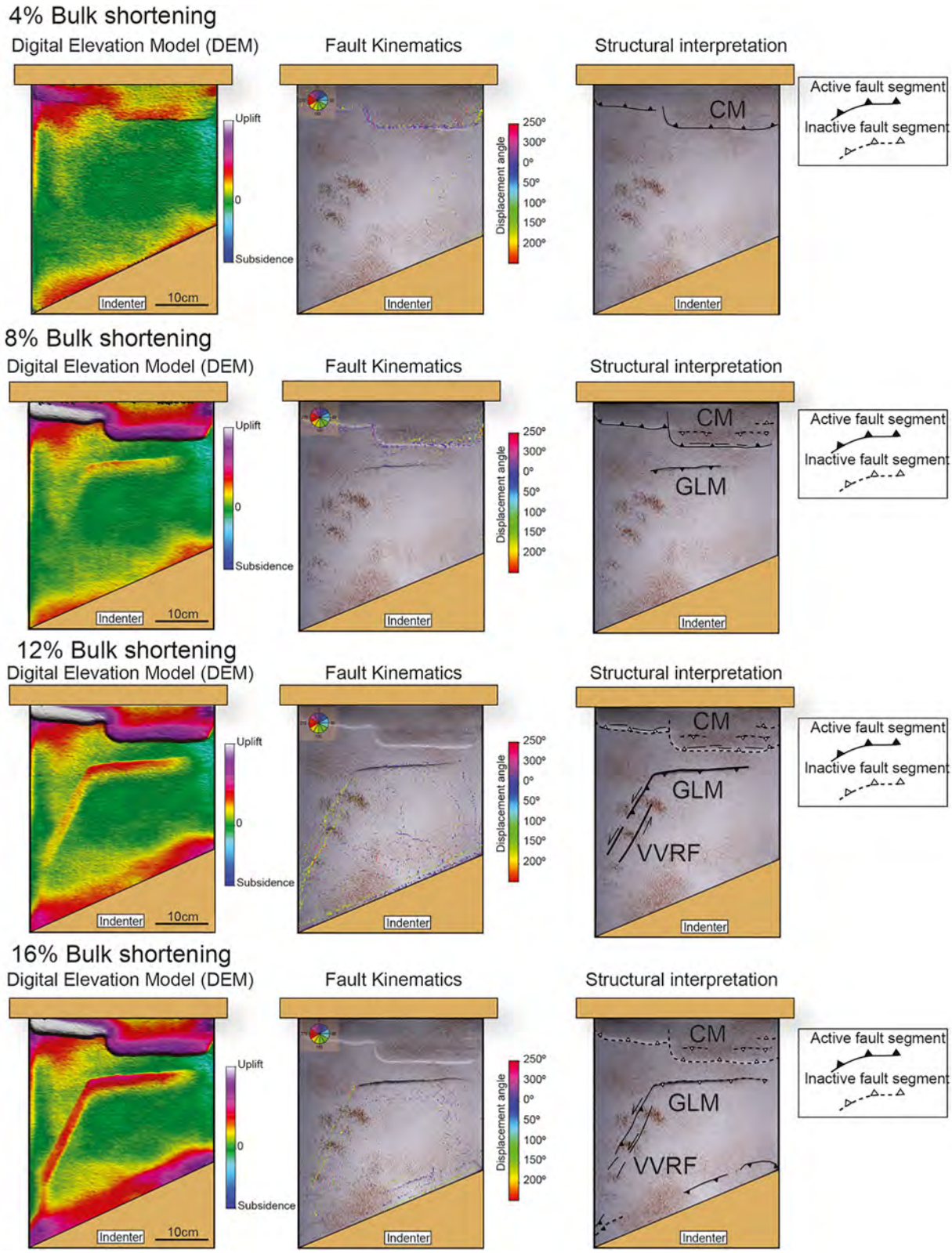

Figure 4. Sandbox experiment showing the evolution of the model topography, the particle image velocimetry field (based on fault kinematics or vector slip is indicated in degrees by the color wheel) and structural interpretation at different stages of deformation.

ble 1). The experiments comprised two steps: (i) a first step using a plastic sheet that was pulled against a wood indenter (Figure 3) to cause shortening, representing the N-S compression as occurred during the collision between the European and Iberian plates (Pyrenean stage, Figure 2a) and (ii) Shortening produced by a moving wall indenter pushing from the southern border of the model (Betic stage, Figure 2b). The model was shortened by 16% of total bulk shortening (Figure 4), according to rates of alpine shortening suggested by Alonso et al. (1996).

The physical properties and scaling parameters to account for geometric and dynamic similarities were obtained through dimensional analysis based on the Ramberg Number and Smoluchowski Number for the viscous and brittle behavior, respectively, (Table 1) according to Ramberg (1967), Weijermars and Schmeling (1986) and Brun (1999):

$$\sigma* = \rho * g * L *$$

where σ refers to stress, ρ to density, g to gravitational acceleration, and L to the length scale. The asterisk refers to the ratio between model and nature, the dimensionless ratio. Since in our study g* equals one and the densities of the used silicon putties (~1300–1356 kg m^{-3}) and rocks in nature (2750–2900 kg m^{-3}) are in the same order of magnitude, we can assume that $\sigma* = L*$. Therefore, considering the physical material properties and their equivalents in nature, the stress ratio of 3.25×10^{-7}, which implies a geometric scaling of 1 cm in the model to 10 km in nature (i.e., vertical and horizontal).

Finally, the topographic uplift was recorded using a laser scanner to obtain a digital elevation model during the deformation of the experiments. Comparison of time-lapse digital models aimed at the interpretation of active faulting and uplift (Figure 4).

3.2. Particle Image Velocimetry (PIV)

The analysis of fault kinematics carried out on the model surface was implemented following the methodology described in Leever et al. (2011) and Fernández-Lozano et al. (2019). Their method is based on the study of the particle displacement field performed over the surface of the experiments. The PIV method compares two images within a fixed time interval. The image evaluation is carried out by dividing the PIV recording into several small subareas, the so-called interrogation windows. The record is measured in picture elements or pixels. Therefore, if small-grain particles are scattered over the model surface, those particles within the interrogation areas will be correlated.

Evaluation of PIV recordings was obtained by cross-correlation method, defined as a standard statistical method of estimating the degree to which two compared series of data were correlated (Raffel et al., 2004; Westerweel et al., 1997). The PIV method aimed to investigate fault slip by comparing the velocity field and slip orientation between models during deformation.

3.3. Brittle-Ductile Transition Zone and Yield Strength Maps

The BDTZ and yield strength maps were carried out (Figure 5) based on the structural surface pattern and the deep structure of the analog experiment. After deformation, the model was cut along N-S profiles subparallel with the shortening direction. Sixteen profiles were acquired and digitized using pictures of every cross-section. These profiles were used to generate the contour map of Figure 5b. In our analog experiments, the BDTZ is represented by the sand-silicone boundary.

The BDTZ was generated by digitizing every cross-section after deformation, assuming the scaling ratio 1:10 (see scaling parameters in Table 1). The digitized surfaces were interpolated using a kriging algorithm in Golden Surfer 10®. The interpolated map generated consists of a Digital Model with depth contours of the BDTZ, providing an estimation of the thickness of the seismogenic layer from the model.

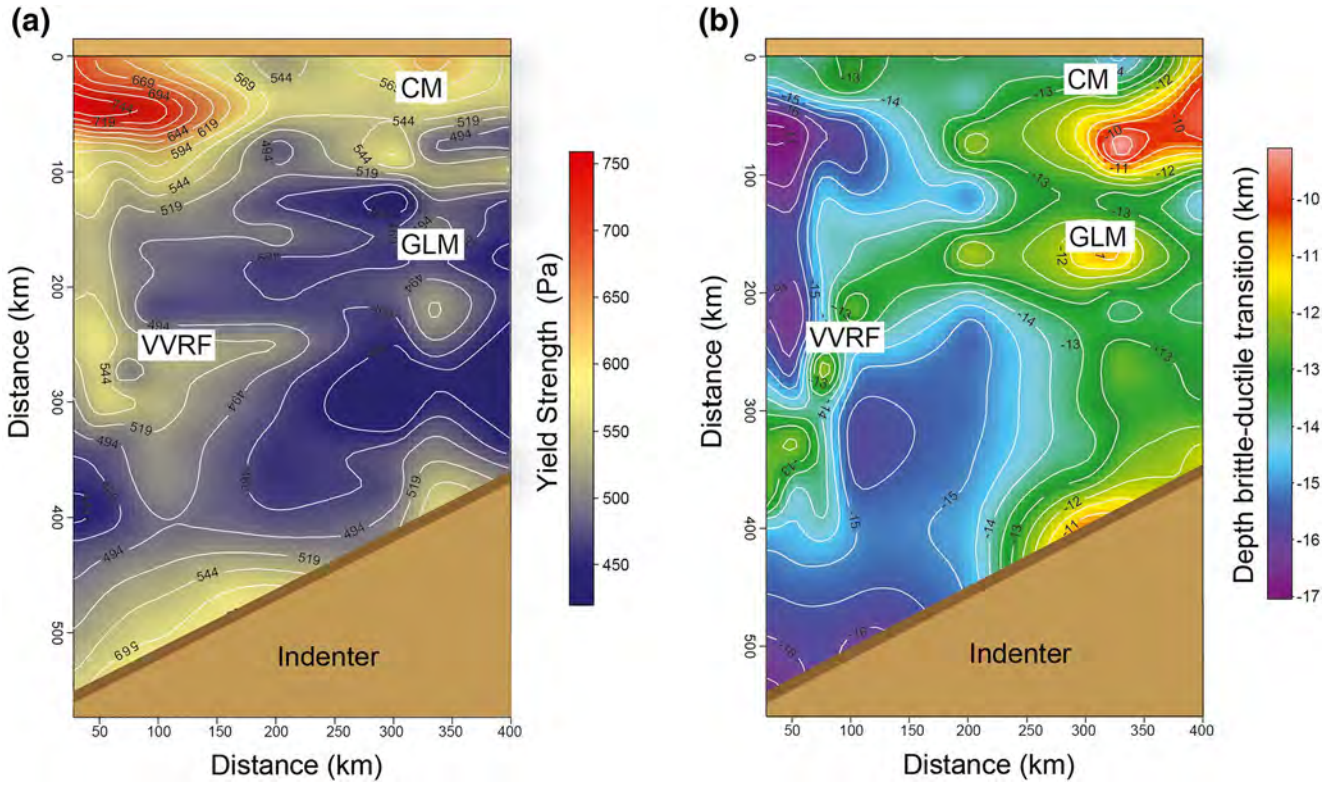

Figure 5. a) Yield strength (Pa) and (b) BDTZ maps of the sandbox experiment showing the correlation between thickened regions and high strength areas of the model's crust.

The differential stress or yield stress (ψ) for the brittle crust was determined following the Byerlee's fracture criterion (Byerlee, 1978) under compression using the method previously reported in Fernández Lozano et al. (2010) and given by the relation:

$$\psi = \frac{\left(2 * \mu * \rho * g * h\right) + \left(2 * C_o\right)}{\left(\mu^2 + 1\right)^{1/2} - \mu}$$

where μ refers to the coefficient of friction, ρ to density, g to gravity, h to layer thickness, and C_o represents the cohesion in Pascals (See Table 1).

4. Modeling Results

The experiment was performed using four weak zones. Two E-W initial weak zones to observe the control of the Cantabrian mountains and the Galaico-leonese mountains main thrusts, an NNE-SSW weak zone that represents the NNE-SSW structures (compare Figures 2b and 4) and the Cantabrian Arc. Shortening orientation shifted during the running of the experiment, from an early N-S phase (after 8% shortening) to a subsequent second phase trending SSE-NNW. This second phase of deformation in the model was based on the shift that was activated during shortening applied using an indenter from the south (Figure 3).

During the first steps of deformation (4% bulk shortening), the model front along the pulling wall was activated. The Western margin was active along the Cantabrian Arc pre-existent weak zone. The fault kinematics analysis shows pure shortening parallel to the N-S direction of compression. This led to active thrusting and elevation along the northern sector of the experiment (see uplift variations in Figure 4). However, uplift

was heterogeneously distributed across strike, probably due to the presence of activity along the pre-existent weak zone.

Shortening from the north gave rise to the nucleation and uplift along the E-W striking weak zone (8% bulk shortening). A north-vergent thrust developed leading to the formation of a minor pop-down and a subsequent intramountain basin. After this step, (12% bulk shortening) the Cantabrian Arch weak zone seems to be inactive according to the fault kinematics analysis. Uplift continues to develop along the active areas. After shifting shortening from the indenter to 12% bulk shortening, the NNE-SSW weak zone reactivated as a left-lateral strike-slip system with a reverse component (see fault kinematics diagram in Figure 4). This defined a left-lateral strike-slip movement along the main structure, leading to a restraining step-over.

At 12% of bulk shortening the northern thrust wedge became inactive. However, the E-W north-vergent thrust and the NNE-SSW step-over nucleated along the weak zones are still active showing important uplift until 16% bulk shortening. As shown in the fault kinematics diagram, the NNE-SSW developed mostly strike-slip movements. At this rate of deformation, the southern border that was slightly uplifted during 8%–12% of bulk shortening started to develop active thrusting leading to an indenter wedge (16% bulk shortening, Figure 4). The final configuration of mountain range uplift was achieved by 16% bulk shortening.

The BDTZ and the yield strength maps of the model obtained after deformation show the contribution of the main tectonic structures to uplift and thickening of the crust. For instance, close to the upper left corner of the model, the yield strength value is highest. This agrees with a deeper position of the BDTZ in the Western upper corner of the model (Figure 5). Likewise, the areas with intermediate topography across the Galician-Leonese Mountains and Verín-Vila Real Fault show also high values of yield strength. This correlation is also observed in those areas of the model where no tectonic activity is recorded, which correspond to smaller values in yield strength.

5. Discussion

In the studied region the thickness of the seismogenic zone (defined by the crust with the 95% of the seismicity, Magistrale, 2002) is about 15–21 km thick (Figure 6). The boundary between the upper- and middle crust in NW Iberia is extended to 12 km, while the Moho discontinuity is estimated to be at 30–32 km (Córdoba et al., 1988; Díaz et al., 2009; Fernández-Viejo et al., 2000; Rodríguez-Fernández et al., 2015). Recent rheological studies carried out in this region suggest that the evidence of a seismogenic zone about 10–16 km deep (i.e. the middle crust) is represented by a sharp seismic boundary from which earthquake activity rapidly vanishes (Figure 1), defining the BDTZ. This zone may correspond with the boundary between upper and lower levels of the crust argued by Llana-Fúnez and López-Fernández (2015). Reflection and refraction data showed that this transition occurs in NW Iberia at depths of 12–20 km with important lateral changes (Fernández-Viejo et al., 2000; Llana-Fúnez & López-Fernández, 2015; Pérez-Estaún et al., 1994; Simancas et al., 2003). It is deeper toward the Southwest (21 km) and shallower in the east (15 km) (Figure 7a). To investigate the mechanisms that govern the BDTZ in this region we have compared the seismogenic thickness with factors that can control its thickness, like total crustal thickness, heat flow, fluid presence and tectonic structures and style (Figure 1).

Comparison with frequency analysis of 2,223 earthquakes collected from the Instituto Geográfico Nacional (IGN, www.ign.es) and the GASPI project (López-Fernández et al., 2004) seismic networks between 1980 and 2016 suggest that the BDTZ in NW Spain reaches a depth of 15–20 km. The upper BDTZ limit corresponds to the cumulative frequency of 10%, which represents depths of 2.5 and 5 km, whereas the lower limit (cumulative frequency of 90%) is about 15 km deep (See Figure 6b). These data are in agreement with previous studies carried out in the area that suggested the BDTZ ranges between 15 and 22 km depth (Llana-Fúnez & López-Fernández, 2015). The analysis of these data onshore, highlights the significant thickening of the crust in the southwestern zone with depths of 21 km in contrast to the minimum recorded in the east where the limit reaches 15 km (Figure 1). On the other hand, the intermediate values are located in the northeast with values around 18–20 km. This implies that the depth of the BDTZ (represented as a sharp rheological discontinuity) is directly influenced by the presence of Alpine tectonic structures and other mechanisms that may govern the lateral-strength variations observed across the BDTZ (Figure 7b).

10.1029/2020TC006493

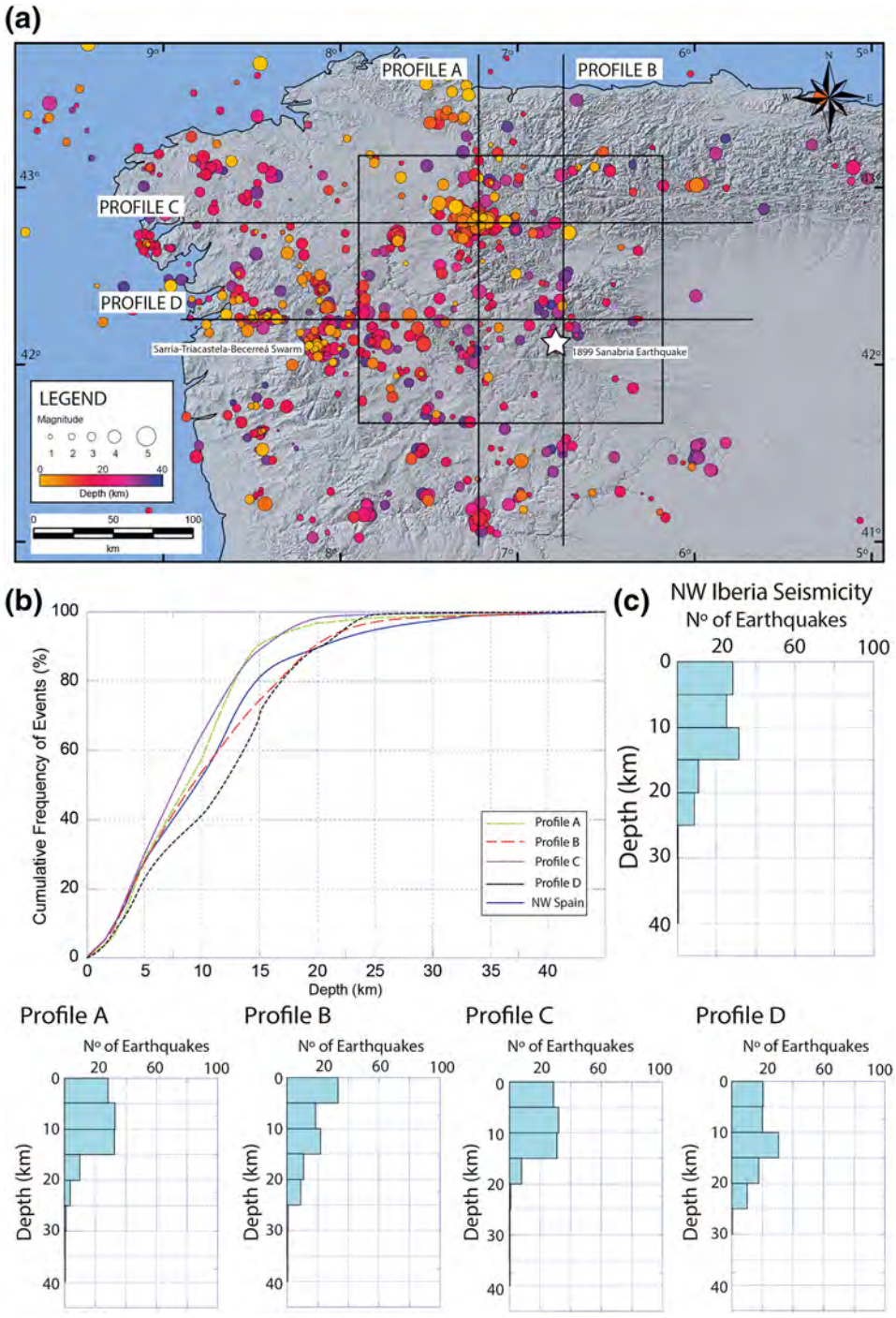

Figure 6. a) Distribution of seismic events in NW Iberia. (b) Cumulative frequency events curve according to depth from different profiles shown in (a). (c) Total seismicity in NW Spain and across profiles A; B; C, and D. Seismic data from IGN (www.ign.es) and GASPI Project from 1980 to 2016.

Analog experiments provide an excellent approach to explore the structural framework, kinematics, tectonic styles, and the upper crustal thickness variations of plate interiors. The BDTZ map obtained from the sandbox experiment shows a strong correlation with the location of thrust planes at depth and, therefore, with the observed seismogenic crustal thickness variations (compare Figures 7a and 7b). This relation is also suggested by the yield strength map. It shows the increase of crustal strength in the brittle crust across

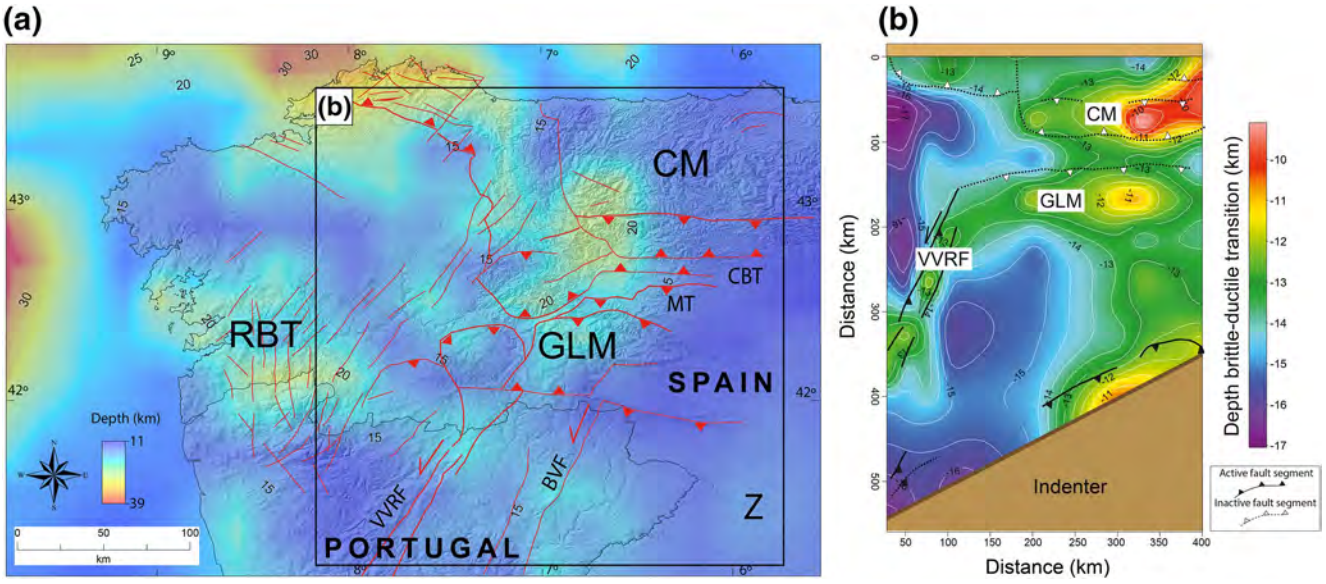

Figure 7. a) BDTZ map of NW Iberia showing the distribution of main Alpine structures referred in the text. Shallow seismicity is shown in the Zamora region (Z) indicating a reduction of depth to the BDTZ (<15 km) toward the south east of the study area. Inset shows the area covered by analog experiment in (b), and (b) BDTZ map of the model (generated from the sandbox cross-sections) and location of active/inactive faults after deformation indicating the relationship between the depth to the BDTZ and the main structures.

areas where the crustal thickness deepens (Figures 5a and 5b). To be able to explain this behavior, other factors such as raising pore pressure due to the presence of fluids circulating through fault planes and high thermal gradients must be invoked to play an important role on the brittle failure of the crust. This interaction is also observed in Iberia as depicted in Figure 1. Striking variations are mainly E-W trending areas located in the north and northeast, related to the main Alpine structures that are E-W thrusts detached in the middle crust, which uplift the upper crust and represent the Cantabrian Mountains and Galaico-Leonese Mountains structures (Figure 7b). These tectonic areas show a strong correlation with the BDTZ variations defined for the NW of the Iberian Peninsula and, therefore, with the tectonic evolution and structures in the region (Figures 4 and 7). A good example is shown in the Zamora sector. In this area, the BDTZ is located at shallow depths (<15 km) and is associated with the reactivation of an Alpine thrust that uplifted the basement leading to a rough surface topography in the area (Figure 7a). This tectonic behavior may account for the observed differences in river incision argued by Antón et al. (2015) associated with shallow structures that may have been inherited from the Late-Variscan orocline-related deformation (Fernández-Lozano et al., 2019). These structures have played a key role on landscape change by facilitating rapid erosion and exhumation, which in turn may have influenced a rapid variation in BDTZ depth in the western Duero Basin reflected in the seismic behavior of the area (Figure 7a, area marked by Z).

The presence of these thrust faults at depth may account for the circulation of fluids responsible for decreasing the yield strength of the crust, giving rise to significant seismic activity in the area with earthquakes like the one in Puebla de Sanabria in 1899 with Intensity V and estimate magnitude $M = 5.9$ (Figure 6a). Therefore, active thrusting and strike-slip faults in combination with deep fluids—among other factors—can be responsible of the lateral variations and depth of the BDTZ as suggested by the results shown in Figure 7b.

The studied region is known for the existence of deep crustal and even mantellic fluids (Pérez et al., 1996; Rodríguez-Fernández et al., 2015) and it is one of the proposed factors to explain the anomalous seismogenic layer thickness in the NW Iberian Peninsula (Llana-Funez and Lopez, 2015). The existence of these fluids is directly associated with fault length and depth, allowing for deep circulation and increasing fluid pressure.

The anomalous thickness and lateral-strength variations from the BDTZ depth in NW Iberia is the result of a complex combination of different factors. This anomalous thickness suggests the relevance of combined

fluid pressure and lateral-strength variations to influence the location of thrust and fault planes in the crust, generating a more permeable areas for fluid migration. The presence of crustal-scale faults may account for circulating fluids in depth. The latter are thought to be responsible for increasing pore pressure, which contributes to reduce the yield strength of the crust, giving rise to significant seismic activity in the area. Thus, high geothermal gradients in NW Iberia together with the crustal thickness is unlikely to explain all the observed variations in the BDTZ depth.

6. Conclusions

The Galaico-Leonese Mountains in NW Iberia comprised a two-step evolution related to N-S (Pyrenean) and NW-SE (Betic) Alpine shortening. This tectonic shift led to reactivation of pre-existing Late-Variscan structures, which controlled crustal thickening and seismicity in the area. Seismicity is widely distributed to about a depth of 15–20 km suggesting the presence of a seismogenic transition zone between the brittle and ductile crust. The anomalous thickness and lateral-strength variations of the BDTZ depth in NW Iberia is the result of a combination of different factors. The presence of fluids could contribute to increase the thickness of the seismogenic crust in the region. Because fluids can travel through crustal faults increasing pore pressure, they can be responsible for the lateral variations of the BDTZ, giving rise to a significant seismic activity in the area. Analog experiments represent an excellent opportunity to understand depth changes observed along the BDTZ and yield strength during present-day deformation otherwise inaccessible to direct observation.

Data Availability Statement

Datasets comprising the catalog of earthquakes from 1980 to 2016 used for this research are available in these in-text data citation references and websites: López-Fernández, et al., 2004 [López-Fernández, C., Pulgar, J., Gallart, J., Díaz, J., GonzálezCortina, J., Ruíz, M., 2004. Present seismicity and tectonics in the NW Iberian Peninsula (Spain): results from the GASPI project. Geophysical Research Abstracts, 6, EGU04-A-04142-1] and the IGN website [www.ign.es].

Acknowledgments
Authors are indebted to the Utrecht Tec-Lab (The Netherlands) and its crew for assistance during the modeling tasks. This work was partially supported by the Spanish Ministry of Economy and Competitiveness and FEDER (project CGL2015-70970-P) and MARIBNO Project, Ministry of Science, Innovation and Universities PGC2018-095999-B-I00.

References

Alonso, J., Pulgar, J., García-Ramos, J., & Barba, P. (1996). W5 tertiary basins and alpine tectonics in the Cantabrian mountains (NW Spain). Tertiary basins of Spain: The stratigraphic record of crustal kinematics. *Cambridge University Press*, 214–227. https://doi.org/10.1017/CBO9780511524851.031

Andeweg, B. (2002). Cenozoic tectonic evolution of the Iberian Peninsula causes and effects of changing the stress field. *Dissertation*. VU University Amsterdam.

Antón, L., Mather, A. E., Stokes, M., Muñoz-Martin, A., & de Vicente, G. (2015). Exceptional river gorge formation from unexceptional floods. *Nature Communications*, *6*, 7963. https://doi.org/10.1038/ncomms8963

Brun, J. (1999). Narrow rifts versus wide rifts: Inferences for the mechanics of rifting from laboratory experiments. *Philosophical Transactions-Royal Society of London Series A Mathematical Physical and Engineering Sciences*, 695–709.

Byerlee, J. (1978). The friction of rocks. *Pure and Applied Geophysics*, *116*, 615–626.

Cabral, J. (1989). An example of intraplate neotectonic activity, Vilariça Basin, northeast Portugal. *Tectonics*, *8*, 285–303. https://doi.org/10.1029/TC008i002p00285

Córdoba, D., Banda, E., & Ansorge, J. (1988). P-wave velocity-depth distribution in the Hercynian crust of northwest Spain. *Physics of the Earth and Planetary Interiors*, *51*, 235–248.

De Lis Mancilla, F., & Diaz, J. (2015). High-resolution Moho topography map beneath Iberia and Northern Morocco from receiver function analysis. *Tectonophysics*, *663*, 203–211.

De Vicente, G., & Vegas, R. (2009). Large-scale distributed deformation-controlled topography along the western Africa–Eurasia limit: Tectonic constraints. *Tectonophysics*, *474*(1–2), 124–143.

De Vicente, G., Vegas, R., Cabral, J., Van Wees, J. D., & Olaiz, A. (2008). Corredores de desgarre cenozoicos en la Península Ibérica. Geotemas. VII Congreso Geológico de España. *Las Palmas*, *10*, 334–336.

De Vicente, G., Vegas, R., Martín, A. M., Silva, P., Andriessen, P., Cloetingh, S., et al. (2007). Cenozoic thick-skinned deformation and topography evolution of the Spanish Central System. *Global and Planetary Change*, *58*, 335–381.

Dewey, J. F., Helman, M. L., Turco, E., Hutton, D. H. W., & Knott, S. D. (1989). Kinematics of the western Mediterranean. In M. P. Coward, D. Dietrich, & R. G. Park (Eds.), *Alpine tectonics* (pp. 265–283). Geological Society Special Publications.

Díaz, J., & Gallart, J. (2009). Crustal structure beneath the Iberian Peninsula and surrounding waters: A new compilation of deep seismic sounding results. *Physics of the Earth and Planetary Interiors*, *173*, 181–190. https://doi.org/10.1016/j.pepi.2008.11.008

Diaz, J., Gallart, J., & Carbonell, R. (2016). Moho topography beneath the Iberian-Western Mediterranean region mapped from controlled source and natural seismicity surveys. *Tectonophysics*, *692*, 74–85. https://doi.org/10.1016/j.tecto.2016.08.023

Díaz, J., Gallart, J., Pulgar, J., Ruiz, M., & Pedreira, D. (2009). Crustal structure beneath North-West Iberia imaged using receiver functions. *Tectonophysics*, *478*, 175–183.
Duque, M. R. A. (2020). Numerical simulations of terrestrial heat flow in the beiras region, Mainland Portugal. *International Journal of Terrestrial Heat Flow and Applied Geothermics*, *3*(1), 32–37. https://doi.org/10.31214/ijthfa.v3i1.48
Fernández Lozano, J., Sokoutis, D., Willengshofer, E., Muñoz Martín, A., Vicente, G. D., & Cloetingh, S. (2010). Sobre el origen de la asimetría en el patrón general del relieve en el interior de la Península Ibérica: Nuevos resultados obtenidos mediante modelación análoga. *Geogaceta*, (*49*), 67–70.
Fernàndez, M., Marzán, I., Correia, A., & Ramalho, E. (1998). Heat flow, heat production, and lithospheric thermal regime in the Iberian Peninsula. *Tectonophysics*, *291*((1-4)), 29–53. https://doi.org/10.1016/S0040-1951
Fernández-Lozano, J., Gutiérrez-Alonso, G., Willingshofer, E., Sokoutis, D., de Vicente, G., & Cloetingh, S. (2019). Shaping of intraplate mountain patterns: The Cantabrian orocline legacy in Alpine Iberia. *Lithosphere*, *11*(5), 708–721.
Fernández-Viejo, G., Gallart, J., Pulgar, J. A., Córdoba, D., & Dañobeitia, J. J. (2000). Seismic signature of variscan and alpine tectonics in NW Iberia: Crustal structure of the Cantabrian mountains and Duero Basin. *Journal of Geophysical Research*, *105*, 3001–3018. https://doi.org/10.1029/1999JB900321
Gallastegui, J. (2000). Estructura cortical de la cordillera y margen continental cantábricos: perfiles ESCI-N. *Trabajos de Geología*, (22), 3–234.
Gans, P., Miller, E., McCarthy, J., & Ouldcott, M. (1985). Tertiary extensional faulting and evolving ductile-brittle transition zones in the northern Snake Range and vicinity: New insights from seismic data. *Geology*, *13*, 189–193.
Gougb, D. I. (1986). Seismic reflectors, conductivity, water and stress in the continental crust. *Nature*, *323*, 11.
Jiménez-Díaz, A., Ruiz, J., Villaseca, C., Tejero, R., & Capote, R. (2012). The thermal state and strength of the lithosphere in the Spanish Central System and Tajo Basin from crustal heat production and thermal isostasy. *Journal of Geodynamics*, *58*, 29–37.
Karato, S. I. (2012). *Deformation of earth materials: An introduction to the rheology of solid earth*. Cambridge University Press.
Leever, K. A., Gabrielsen, R. H., Sokoutis, D. & Willingshofer, E. (2011). The effect of convergence angle on the kinematic evolution of strain partitioning in transpressional brittle wedges: Insight from analogue modelling and high-resolution digital image analysis. *Tectonics*, *30*. https://doi.org/10.1029/2010TC002823
Llana-Fúnez, S., & López-Fernández, C. (2015). The seismogenic zone of the continental crust in Northwest Iberia and its relation to crustal structure. *Tectonics*, *34*, 1751–1767. https://doi.org/10.1002/2015TC003877
Long, L. T., & Zelt, K. H. (1991). A local weakening of the brittle-ductile transition can explain some intraplate seismic zones. *Tectonophysics*, *186*, 175–192.
López-Fernández, C., Díaz, J., Gallart, J., Pulgar, J., Ruiz, M., & González-Cortina, J. (2012). Seismotectonic characterization of the Becerreá area (NW Spain). *Geológica Acta*, *10*, 0071.-0080.
López-Fernández, C., Pulgar, J., Gallart, J., Díaz, J., GonzálezCortina, J., & Ruíz, M. (2004). Present seismicity and tectonics in the NW Iberian Peninsula (Spain): Results from the GASPI project. *Geophysical Research Abstracts*, *6*, EGU04-A-04142–1.
Maggi, A., Jackson, J., Mckenzie, D., & Priestley, K. (2000). Earthquake focal depths, effective elastic thickness, and the strength of the continental lithosphere. *Geology*, *28*, 495–498.
Magistrale, H. (2002). Relative contributions of crustal temperature and composition to controlling the depth of earthquakes in southern California. *Geophysical Research Letters*, *29*(10), 87–81. https://doi.org/10.1029/2001GL014375
Martín-González, F. (2009). Cenozoic tectonic activity in a Variscan basement: Evidence from geomorphological markers and structural mapping (NW Iberian Massif). *Geomorphology*, *107*, 210–225.
Martín-González, F., Antón, L., Insua, J., De Vicente, G., Martínez-Díaz, J. J., Muñoz-Martín, A., et al. (2012a). Seismicity and potencially active faults in the northwest and central-west Iberian Peninsula. *Journal of Iberian Geology*, *38*, 53.
Martín-González, F., & Heredia, N. (2011a). Geometry, structures and evolution of the western termination of the Alpine-Pyrenean Orogen reliefs (NW Iberian Peninsula). *Journal of Iberian Geology*, *37*, 103.
Martín-González, F., & Heredia, N. (2011b). Complex tectonic and tectonostratigraphic evolution of an alpine foreland basin: The western Duero Basin and the related tertiary depressions of the NW Iberian Peninsula. *Tectonophysics*, *502*, 75–89.
Martínez-Díaz, J., Capote, R., Tsige, M., Villamor, P., Martín-González, F., & Insua-Arévalo, J. (2006). Seismic triggering in a stable continental area: The Lugo 1995–1997 seismic sequences (NW Spain). *Journal of Geodynamics*, *41*, 440–449.
Martín-González, F., Barbero, L., Capote, R., Heredia, N., & Gallastegui, G. (2012b). Interaction of two successive alpine deformation fronts: Constraints from low temperature thermochronology and structural mapping (NW Iberian Peninsula). *International Journal of Earth Sciences*, *101*, 1331–1342. https://doi.org/10.1007/s00531-011-0712-9
Martín-González, F., Freudenthal, M., Heredia, N., Martín-Suárez, E., & Rodríguez-Fernández, L. R. (2014). Paleontological age and correlations of the tertiary of the NW Iberian Peninsula: The tectonic evolution of a broken foreland basin. *Geological Journal*, *49*, 15–27. https://doi.org/10.1002/gj.2484
Martínez-Catalán, J. R., Arenas, R., Díaz García, F., & Abati, J. (1997). Variscan accretionary complex of Northwest Iberia; terrane correlation and succession of tectonothermal events. *Geology*, *25*, 1103–1106.
Marzan, I. (2000). Régimen térmico en la Península Ibérica. Estructura litosférica a través del macizo ibérico y el margen surportugués. Doctoral dissertation, Ph. D. thesis, Barcelona, 181 pp.
Muñoz, J. A. (2002). Alpine tectonics I: The alpine system north of the beltic Cordillera: The Pyrenees. In W. Gibbons, & T. Moreno (Eds.), *The geology of Spain* (pp. 370–385). London: Geological society.
Pérez-Estaún, A., Pulgar, J., Banda, E., Álvarez-Marrón, J., & Group, E.-N. R. (1994). Crustal structure of the external variscides in northwest Spain from deep seismic reflection profiling. *Tectonophysics*, *232(1-4)*, 91–118. https://doi.org/10.1016/0040-1951(94)90078-7
Pérez, N. M., Nakai, S., Wakita, H., Albert-Beltrán, J. F., & Redondo, R. (1996). Preliminary results on $^{3}He/^{4}He$ isotopic ratios in terrestrial fluids from Iberian Peninsula: Seismotectonic and neotectonic implications. *Geogaceta*, *20*, 830–833.
Pollard, D. D., & Fletcher, R. C. (2005). *Fundamentals of structural geology*. Cambridge University Press.
Pulgar, J. A., Gallart, J., Fernández-Viejo, G., Pérez-Estaún, A., Álvarez-Marrón, J., & Escin Group (1996). Seismic image of the Cantabrian Mountains in the western extension of the Pyrenees from integrated ESCIN reflection and refraction data. *Tectonophysics*, *264*((1-4)), 1–19. https://doi.org/10.1016/S0040-1951
Raffel, M., Richard, H., Ehrenfried, K., Van der Wall, B., Burley, C., Beaumier, P., et al. (2004). Recording and evaluation methods of PIV investigations on a helicopter rotor model. *Experiments in Fluids*, *36*, 146–156.
Ramberg, H. (1967). *The earth's crust as studied by centrifuged models*. New York: Academic Press.
Ribeiro, A., Kullberg, M. C., Kullberg, J. C., Manuppella, G., & Phipps, S. (1990). A review of alpine tectonics in Portugal-foreland detachment in basement and cover rocks. *Tectonophysics*, *184*, 357–366.

Roca, E., Muñoz, J. A., Ferrer, O., & Ellouz, N. (2011). The role of the Bay of Biscay Mesozoic extensional structure in the configuration of the Pyrenean orogen: Constraints from the MARCONI deep seismic reflection survey. *Tectonics*, *30*(2), 1–33. https://doi.org/10.1029/2010TC002735

Rockwell, T., Fonseca, J., Madden, C., Dawson, T., Owen, L. A., Vilanova, S., et al. (2009). Paleoseismology of the vilariça segment of the Manteigas-bragança fault in northeastern Portugal. In K. Reicherter, A. M. Michetti, & P. G. Silva (Eds.), Palaeoseismology: Historical and prehistorical records of earthquake ground effects for seismic hazard assessment. Geol. Soc. London. 316 (237–258) Special Publications. https://doi.org/10.1144/SP316.15

Rodríguez-Fernández, L., Pedrera, A., Pous, J., Ayala, C., González-Menéndez, L., Ibarra, P., et al. (2015). Crustal structure of the South-western termination of the alpine Pyrenean–Cantabrian orogen (NW Iberian Peninsula). *Tectonophysics*, *663*, 322–338.

Rosenbaum, G., Lister, G., & Duboz, C. (2002). Relative motions of Africa Iberia and Europe during alpine orogeny. *Tectonophysics*, *359*, 117–129.

Santanach, P. (1994). Las cuencas terciarias gallegas en la terminación occidental de los relieves pirenaicos. *cuaderno laboratorio xeolóxico de laxe*, *19*, 57–71.

Scholz, C. (1988). The brittle-plastic transition and the depth of seismic faulting. *Geologische Rundschau*, *77*, 319–328.

Scholz, C. H. (2002). *The mechanics of earthquakes and faulting*. Cambridge university press.

Sibson, R. (1977). Fault rocks and fault mechanisms. *Journal of the Geological Society*, *133*, 191–213.

Sibson, R. H. (2007). An episode of fault-valve behaviour during compressional inversion?—The 2004 MJ6. 8 Mid-Niigata Prefecture, Japan, earthquake sequence. *Earth and Planetary Science Letters*, *257*((1-2)), 188–199. https://doi.org/10.1016/j.epsl.2007.02.031

Simancas, J., Carbonell, R., González Lodeiro, F., Pérez Estaún, A., Juhlin, C., Ayarza, P., et al. (2003). Crustal structure of the transpressional variscan orogen of SW Iberia: SW Iberia deep seismic reflection profile (IBERSEIS). Tectonics 22.

Stewart, M., Holdsworth, R. E., & Strachan, R. A. (2000). Deformation processes and weakening mechanisms within the frictional–viscous transition zone of major crustal-scale faults: Insights from the great glen fault zone, Scotland. *Journal of Structural Geology*, *22*(5), 543–560.

Suriñach, E., & Vegas, R. (1988). Lateral inhomogeneities of the Hercynian crust in central Spain. *Physics of the Earth and Planetary Interiors*, *51*, 226–234.

Tullis, J., & Yund, R. A. (1977). Experimental deformation of dry westerly granite. *Journal of Geophysical Research*, *82*, 5705–5718.

Vegas, R., de Vicente, G., Muñoz Martín, A., & Palomino, R. (2004). Los corredores de fallas de Regua-Verin y Vilariça: Zonas de transferencia de la deformación intraplaca en la Península Ibérica VI Congreso Geológico de España. *Zaragoza.Geo-temas*, *6*(5), 245–248.

Vergés, J., Kullberg, J. C., Casas-Sainz, A., de Vicente, G., Duarte, L. V., Fernàndez, M., et al. (2019). *An introduction to the alpine cycle in Iberia. In the geology of Iberia: A geodynamic approach*. Cham: Springer. 1-14

Vergés, J., Fernàndez, M., & Martìnez, A. (2002). The Pyrenean orogen: pre-, syn-, and post-collisional evolution. *Journal of the Virtual Explorer*, *8*, 55–74.

Watts, A., & Burov, E. (2003). Lithospheric strength and its relationship to the elastic and seismogenic layer thickness. *Earth and Planetary Science Letters*, *213*, 113–131.

Weijermars, R., & Schmeling, H. (1986). Scaling of Newtonian and non-Newtonian fluid dynamics without inertia for quantitative modeling of rock flow due to gravity (including the concept of rheological similarity). *Physics of the Earth and Planetary Interiors*, *43*, 316–330.

Westerweel, J., Dabiri, D., & Gharib, M. (1997). The effect of a discrete window offset on the accuracy of cross-correlation analysis of digital PIV recordings. *Experiments in Fluids*, *23*, 20–28.